Med Biol Eng Comput (2014) 52:1019–1030
DOI 10.1007/s11517-014-1201-7

ORIGINAL ARTICLE

Adaptive motion artefact reduction in respiration and ECG signals for wearable healthcare monitoring systems

Zhengbo Zhang · Ikaro Silva · Dalei Wu · Jiewen Zheng · Hao Wu · Weidong Wang

Received: 18 May 2013 / Accepted: 22 September 2014 / Published online: 2 October 2014

Abstract Wearable healthcare monitoring systems (WHMSs) have received significant interest from both academia and industry with the advantage of non-intrusive and ambulatory monitoring. The aim of this paper is to investigate the use of an adaptive filter to reduce motion artefact (MA) in physiological signals acquired by WHMSs. In our study, a WHMS is used to acquire ECG, respiration and triaxial accelerometer (ACC) signals during incremental treadmill and cycle ergometry exercises. With these signals, performances of adaptive MA cancellation are evaluated in both respiration and ECG signals. To achieve effective and robust MA cancellation, three axial outputs of the ACC are employed to estimate the MA by a bank of gradient adaptive Laguerre lattice (GALL) filter, and the outputs of the GALL filters are further combined with time-varying weights determined by a Kalman filter. The results show that for the respiratory signals, MA component can be reduced and signal quality can be improved effectively (the power ratio between the MA-corrupted respiratory signal and the adaptive filtered signal was 1.31 in running condition, and the corresponding signal quality was improved from 0.77 to 0.96). Combination of the GALL and Kalman filters can achieve robust MA cancellation without supervised selection of the reference axis from the ACC. For ECG, the MA component can also be reduced by adaptive filtering. The signal quality, however, could not be improved substantially just by the adaptive filter with the ACC outputs as the reference signals.

Keywords Motion artefact · Gradient adaptive Laguerre lattice filter · Kalman filter · Respiration · Wearable healthcare monitoring system

Z. Zhang · H. Wu · W. Wang (✉)
Department of Biomedical Engineering, Chinese PLA (People's Liberation Army) General Hospital, Beijing, China
e-mail: wangwd301@126.com

Z. Zhang · I. Silva
Harvard-MIT Division of Health Sciences and Technology, Massachusetts Institute of Technology, Cambridge, MA, USA

D. Wu
Department of Computer Science and Engineering, The University of Tennessee at Chattanooga, Chattanooga, TN, USA

J. Zheng
Institute of Medical Equipment, National Biological Protection Engineering Centre, Tianjin, China

1 Introduction

In recent years, there has been growing interest in wearable healthcare monitoring systems (WHMSs) in both research and industry. Physiological and psychological data acquired in real life by wearable systems can enable early detection of diseases, reveal correlations between lifestyle and health, and bring healthcare to remote locations and resource-poor settings [31, 36, 43]. In situations where workers are exposed to extreme conditions, dangers or hazards, employing wearable technology can help monitor their vital signs and save their lives [24, 32, 43]. In sports medicine, likewise, unobtrusive wearable sensors can be used to capture physiological data and physical movements of multiple people in real time for the purposes of analysis and performance evaluation [6, 7].

To make these WHMSs practically applicable, however, a series of technical problems need to be overcome. Among them, motion artefact (MA) reduction is one of the most challenging issues, since these wearable systems are mainly used in ambulatory conditions. As biomedical

signals are sensitive to body movement, physiological signals could be badly corrupted by MA caused by variations or movement of the subject. Therefore, robust and effective MA reduction techniques are necessary for solving the MA reduction problem [35, 41].

The spectrum of MA usually overlaps with physiological signals and changes in different movement conditions such as walking, jogging and running. Therefore, traditional digital filters with fixed coefficients in these situations fail to separate MA component from physiological signals effectively. To address this confounding issue, a class of filters known as adaptive digital filters has been developed to achieve optimal filtering. Adaptive filters allow detecting and tracking the dynamic variations of the signals, and alter their filtering characteristic automatically. This type of filter has been shown useful in many biomedical applications [11, 13, 15], e.g. power line interference cancellation in ECG signals [22], and foetal ECG recording by using mother's ECG as a correlated noise source for adaptive noise cancellation [10].

To achieve effective MA cancellation, reference signal and structure of the adaptive filter are of immense significance. Performance of MA cancellation depends on the correlation between the reference signal and the MA component in the contaminated signals. To remove the MA component from ECG signals, Pecht Liu et al. [21] described a method of adaptive MA filtering by using skin strain as a reference signal. Thakor and Zhu [37] developed an adaptive recurrent filter for MA cancellation in ECG recordings, with the generated impulse series coincident with QRS complex as a reference signal. There are also some other reports using the outputs of an accelerometer (ACC) as reference signals for adaptive MA cancellation for ECG signals [20, 29, 38]. Compared with ECG, MA reduction in respiratory signals is sparse in the literature. Recently, performance of different wearable breathing monitoring systems was evaluated in terms of susceptibility to MA [17]. To improve the accuracy of respiratory measurement, Keenan and Wilhelm proposed a least mean square (LMS) adaptive filter for MA cancellation with a triaxial ACC signal as Ref. [16]. In addition, other researches demonstrated the capability of MA reduction in photoplethysmogram (PPG) signals by adaptive filtering with ACC signals as the reference input [18, 28].

Among above-mentioned applications, LMS algorithm was widely used due to its inherent conceptual and implementation simplicity. For LMS algorithm, however, step size needs to be carefully chosen to balance the stability and convergence speed. Meanwhile, it has inherent disadvantage of relatively slow convergence speed due to eigenvalue spread, which will decrease the performance of MA cancellation, when the eigenvalue spread of the input autocorrelation matrix changes during ambulatory monitoring. Furthermore, little attention has been paid to how to achieve robust MA cancellation in physiological signals acquired at different activity levels. For respiratory signals, Keenan's study only showed that ACC signals could be used for adaptive MA cancellation for respiratory signals and only one axial output was utilized. Performance of adaptive filtering for MA cancellation in physiological signals acquired by WHMS at different exercise levels has not been evaluated.

In this paper, performance of adaptive MA cancellation is evaluated in both respiration and ECG signals. A wearable physiological monitoring system was used to acquire respiration and ECG during treadmill and cycle ergometry exercise. A triaxial ACC was integrated in the wearable system to capture the body activities. The outputs of the ACC were used as reference signals for adaptive MA cancellation. Rather than employing only single channel of the ACC output as reference input, three axial outputs of the ACC were all used for MA estimation by a bank of gradient adaptive Laguerre lattice (GALL) filter [8]. The outputs of the GALL filters were further linearly combined by a Kalman filter. This kind of filter structure has been successfully used for physiological waveform prediction and ICU physiological signal quality index estimation [33]. In this study, the Kalman filter adaptively adjusts its weights to achieve robust MA cancellation by combing multiple channels of MA estimation from the ACC signals.

2 Materials and methods

2.1 Materials

Dataset used for this study was collected during treadmill and cycle ergometry exercises by a wearable monitoring system called Sensing Shirt [44]. The study was reviewed and approved by the Ethics Committee of Chinese PLA General Hospital. Ten healthy volunteers (without respiratory and heart diseases, ageing from 22 to 32) participated in this experiment with given prior and informed consent. Physiological signals of rib cage (RC) and abdomen (AB) motions, single-lead ECG and triaxial ACC (Axis I, Axis II and Axis III) were recorded. During the experiment, each subject firstly performed an incremental treadmill test, including four stages of stationary standing (0 km/h), walking (4 km/h), jogging (6 km/h) and running (8 km/h). Each stage lasted about 2 min. Secondly, the subject completed an incremental cycle ergometry exercise, which also had four stages of sitting (0 rpm), slow pedalling (20 rpm), medium pedalling (30 rpm) and fast pedalling (40 rpm). Each stage also lasted about 2 min.

Figure 1 shows the physiological waveforms and each axial output of the ACC captured by the Sensing Shirt

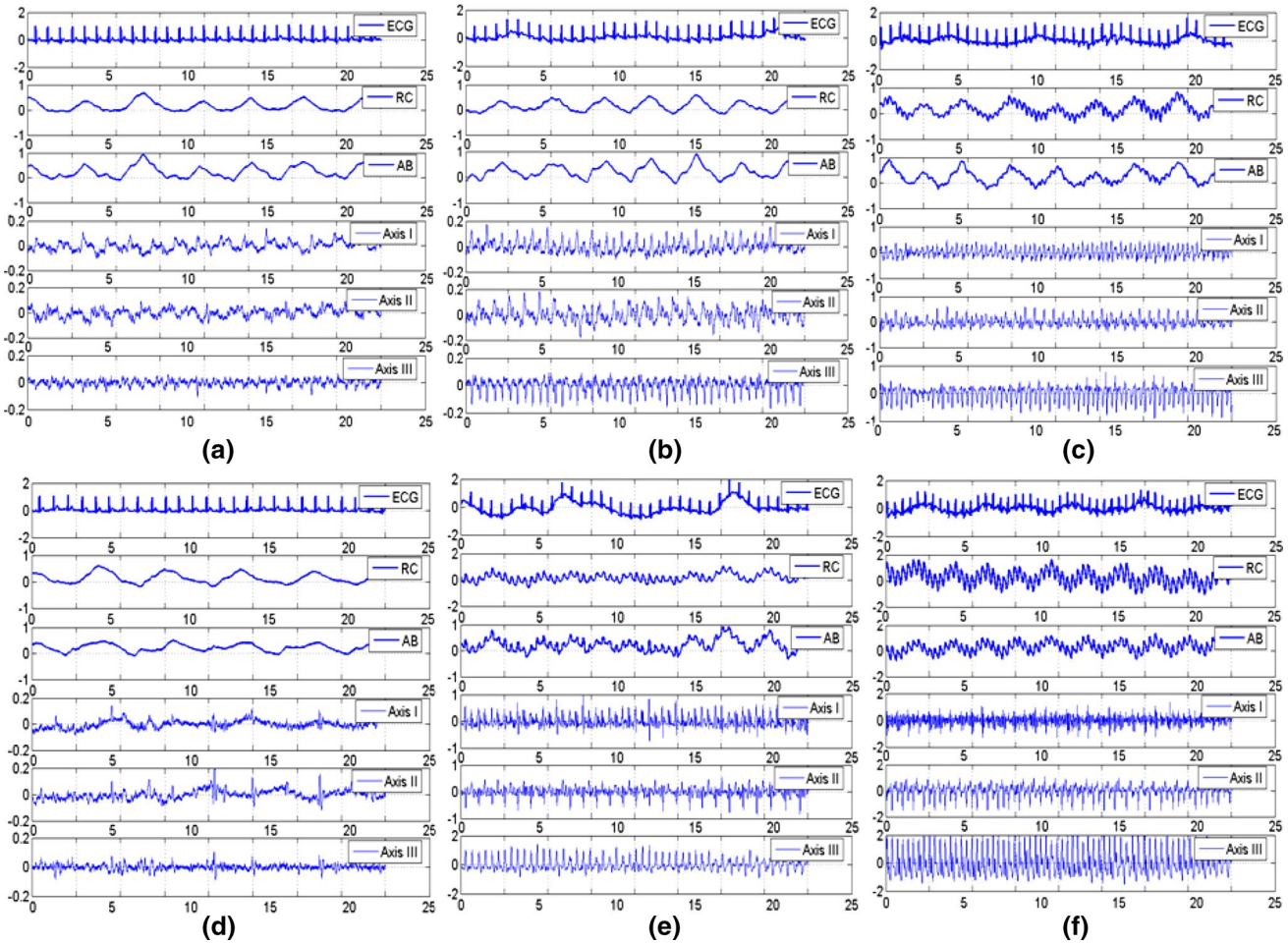

Fig. 1 Physiological signals captured by Sensing Shirt at different activity levels (**a** slow pedalling, **b** medium pedalling **c** fast pedalling, **d** walking, **e** jogging, **f** running). In each sub-figure, ECG is displayed in the first trace. Below are the traces of RC, AB, Axis I, Axis II and Axis III

during the incremental treadmill and cycle ergometry exercise from one subject. In the Sensing Shirt, ECG (Lead II) is acquired by using Ag–AgCl electrodes for bio-potential detection. Active electrodes are integrated in the electrodes to acquire high-quality signals for ambulatory monitoring. Two channels of respiratory movement (RC and AB) are recorded by respiratory inductive plethysmography (RIP) [42]. Specifically, two RIP sensors in parallel sinusoidal arrays of insulated wires embedded in elastic bands are woven into the shirt around the chest and AB. One triaxial ACC, MMA7260, is integrated in the shirt to capture body posture and activities. The ACC is mounted on a printed circuit board packaged in a small box which is placed in one front pocket on the shirt. In the experiment, ECG, RC and AB motions, and the triaxial outputs of the ACC were all sampled at 200 Hz for adaptive signal processing.

It has been demonstrated that for RIP, the sum of RC and AB outperforms individual use of RC or AB for breath detection [5]. Therefore, in our study, RC and AB displacements were linearly combined with unit coefficients to represent the respiratory movement during exercise [2].

2.2 Adaptive MA filtering

Adaptive filtering involves change of filter parameters over time to adapt to dynamic signal characteristics. In MA cancellation, the corrupted signal combines the MA component and desired information. To remove the MA component, a signal correlated with the MA is fed to the adaptive filter. So long as the input signal to the filter remains correlated with the MA component in the corrupted signal, the adaptive filter adjusts its coefficients to estimate the MA and result in a relatively clean signal [39]. In essence, MA in physiological signal is caused by body movement. ACC provides a cost-effective and reliable way for body posture and activity recording. Therefore, in our study, the outputs of the triaxial ACC were used as reference inputs to the adaptive filter for MA estimation. The block diagram of

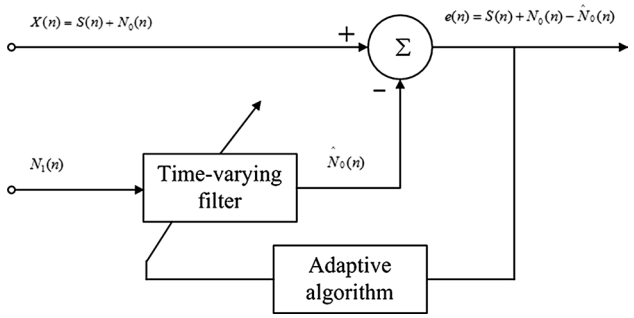

Fig. 2 General configuration of adaptive MA cancellation

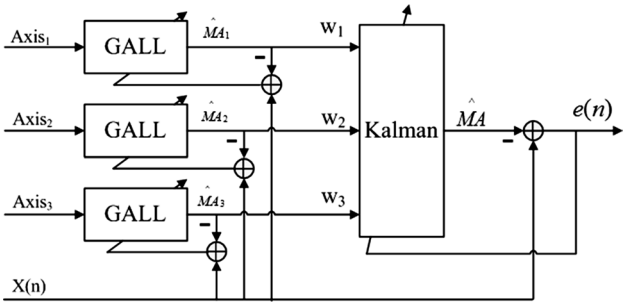

Fig. 3 Overall structure of the adaptive MA estimation and Kalman filter

our approach is shown in Fig. 2, where $X(n)$ represents the physiological variable corrupted by MA component $[N_0(n)]$ during activities, and $N_1(n)$ is one axial output of the ACC, which is highly correlated with the MA component. With a specific adaptive algorithm, the filter adjusts its coefficients to generate optimal estimation of the MA component and achieve a relatively clean signal.

In our study, a bank of GALL filter was used for MA component estimation. The GALL structure combines the desirable features of the Laguerre structure (i.e. guaranteed stability, unique global minimum and fewer parameters to model a linear time-invariant system) with the numerical robustness and low computational complexity of adaptive FIR lattice structures. Furthermore, to achieve a robust MA estimation during different activities, the outputs of the three GALL filters were further combined with time-varying weights determined by a Kalman filter.

2.2.1 *Overall structure*

The overall MA cancellation scheme consists of two stages (Fig. 3). In the first stage, three MA estimates, $\hat{\mathrm{MA}}_m$, are generated by three GALL filters from each axial output of the ACC. In the second stage, these three MA estimates are further linearly combined by an unforced Kalman filter [14] to obtain a robust MA estimation. The final MA estimate made by the Kalman filter is removed from the corrupted physiological signal to recover a relatively clean signal. In Fig. 3, $X(n)$ represents the MA-contaminated physiological recording, $e(n)$ is the relatively clean signal achieved by adaptive filtering.

2.2.2 *GALL filter*

The GALL filter consists of orthogonalizing and joint sections (Fig. 4), in which delays are replaced by Laguerre transfer functions

$$L(z) = \frac{z^{-1} - \alpha}{1 - \alpha z^{-1}}, \tag{1}$$

where the transfer function's pole, α, is constant across the entire filter [8]. The input of the GALL filter is one of the axial outputs of the ACC, and the desired response is the MA-corrupted physiological signal, $X(n)$. In this application, we get three channels of MA estimates with three GALL filters.

2.2.3 *Unforced Kalman filter*

The unforced Kalman filter means unforced space-state model with the process noises zero [14]. As shown in Fig. 3, 3×1 sample-by-sample MA estimates are used as the inputs to the unforced Kalman filter, where the vector

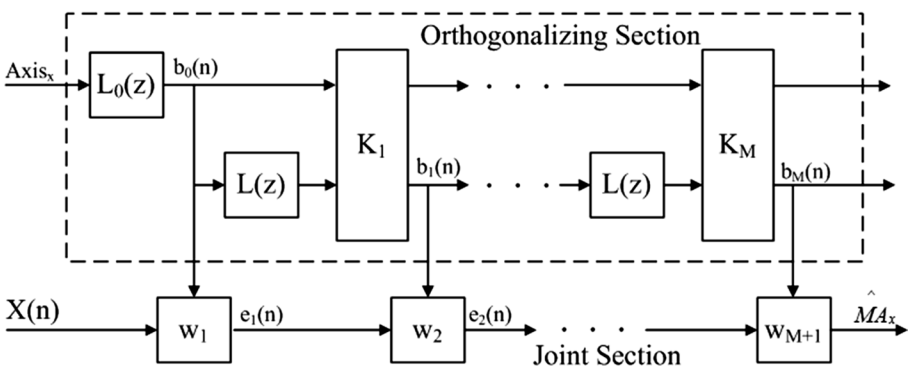

Fig. 4 Overview of the GALL filter

of 3 × 1 weights w is defined as the filter's states and is updated adaptively. The details of the unforced Kalman filter are as follows.

$$u[n] = \left[\hat{\mathrm{MA}}_1[n],\ \hat{\mathrm{MA}}_2[n],\ \hat{\mathrm{MA}}_3[n]\right]^T \tag{2}$$

$$w[n] = [w_1[n], w_2[n], w_3[n]]^T \tag{3}$$

$$\hat{\mathrm{MA}}[n] = u[n]^T \cdot w[n], \tag{4}$$

where $u[n]$ is the vector of the MA estimates, and $w[n]$ is the vector of weights. The weights updating of the unforced Kalman filter are implemented by using the following equations:

$$\varepsilon[n] = x[n] - \hat{\mathrm{MA}}[n] \tag{5}$$

$$g[n] = \frac{\lambda_K^2 K[n-1]u[n]}{u[n]^T K[n-1]u[n] + 1} \tag{6}$$

$$w[n] = \lambda_K w[n-1] + g[n]\varepsilon[n] \tag{7}$$

$$K[n] = \lambda_K^2 K[n-1] - \lambda_K g[n]u[n]^T K[n-1], \tag{8}$$

where λ_K is a scalar forgetting factor between 0 and 1, $K[n]$ is the state error correlation matrix, and $g[n]$ is the Kalman gain.

2.3 Simulation

In the first experiment, simulations were conducted to evaluate the performance of the GALL filter for adaptive MA cancellation by comparing it with the commonly used LMS algorithm. For respiration signals, instead of using Gaussian noise as an additive noise model, we chose one axial output (vertical axis in this case) of the ACC at different activity levels as the noise signals (MA component). One segment of the clean respiratory waveform at standing stage was selected as the original signal. The noise signals passed through an FIR low-pass filter (with a cut-off frequency of 10 Hz and an order of 31) and then were added to the original signal to form MA-contaminated signals. There is not much MA component residing in the respiratory waveforms during walking, slow pedalling and medium pedalling (see it in Fig. 1). Therefore, only three segments of respiratory signals were synthesized with three levels of additive MA component, which were corresponding to fast pedalling, jogging and running, respectively. With these simulation data, the performances of the GALL filter and LMS filter were studied. In the second experiment, the actual respiratory data acquired at different exercise levels were used to test the performance of the algorithm.

For ECG, to simulate the MA component along with other high-frequency noise, Gaussian white noise (with zero mean and unit variance) plus a sine wave was generated as noise (i.e. the reference signal). One segment of the clean ECG at the standing stage was extracted as an original ECG signal. The noise signals were processed in the same way as that in the respiratory simulation section and were added to the original ECG signal to form the MA-contaminated signals.

2.4 Indices for performance evaluation

As the respiratory signals were acquired during exercise, in this study, there was no gold standard measure of respiration for comparison. Furthermore, the aim of our study was to improve respiratory measurement quality, not just for breath rate detection. Therefore, breathing rate detection is not adequate to be a gold standard for this study.

To quantitatively evaluate the MA cancellation performance, the power ratio (PR) between the power of the primary input signal and that of the error signal was used as the evaluation parameter [1].

$$\mathrm{PR} = \frac{E\left[|X(j\omega)|^2\right]}{E\left[|e(j\omega)|^2\right]}, \tag{9}$$

where X represents the FFT of the primary signal and e represents the FFT of the error signal. $E[|\cdot|]$ is the expected value. In adaptive MA cancellation application, the error signal is the desired information.

Recently, the concept of signal quality index has been proposed and used to evaluate signal quality for signals acquired in intensive care unit and ambulatory monitoring [4, 19]. Chen et al. [3] developed a method to estimate respiratory waveform quality based on breath detection over varying baseline values. Nemati et al. [25] proposed using the spectral purity as the respiratory signal quality index. In this study, the effectiveness of the spectral purity index (SPI) in quantifying the respiratory signal quality was evaluated. Furthermore, another signal quality index, spectral distribution ratio (SDR) [19], was defined and used for respiratory signal quality assessment.

SPI is defined as [34]:

$$\mathrm{SPI} = \frac{\overline{\omega_2^2}(k)}{\overline{\omega_0}(k)\overline{\omega_4}(k)}, \tag{10}$$

where the nth-order spectral moment $\overline{\omega_n}$ is defined as:

$$\overline{\omega_n} = \int_{-\pi}^{\pi} \omega^n S_x(e^{j\omega})\mathrm{d}\omega, \tag{11}$$

where $S_x(e^{j\omega})$ is the power spectrum of the signal. In the case of a periodic signal with a single dominant frequency, SPI takes the value of one and approaches to zero for non-sinusoidal noisy signals.

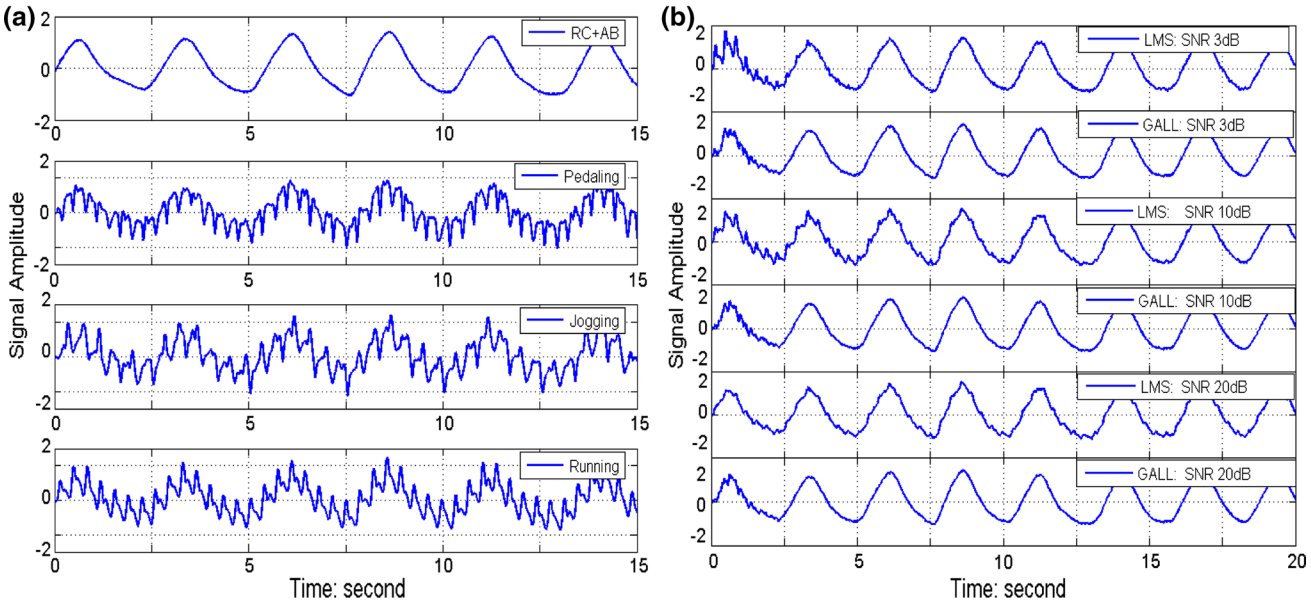

Fig. 5 **a** Clean and synthesized respiratory signals; **b** results of adaptive filtering with LMS and GALL algorithms on the simulation signals with additive MA component at an SNR of 3, 10 and 20 dB, respectively

The SDR of a respiration segment is defined to be the ratio of the sum of the power, $|X(j\omega)|^2$, of the respiration between frequencies, f, of 0.15–1.5 Hz to the power between 1.5 and 10 Hz as follows:

$$\mathrm{SDR} = \frac{\int_{f=0.15}^{f=1.5} |X(j\omega)|^2 \mathrm{d}f}{\int_{f=1.5}^{f=10} |X(j\omega)|^2 \mathrm{d}f} \tag{12}$$

when the SDR is low, more MA component residing in the respiration and the signal quality is bad.

3 Results

3.1 Performance of MA cancellation in respiratory signal

3.1.1 Simulation results

Figure 5a shows the clean respiratory signal and three synthesized respiratory signals with the additive MA components in fast pedalling, jogging and running with an SNR of 3 dB. Figure 5b shows the results of the MA cancellation by both the GALL filter and LMS filter, with additive MA components associated with running stage with an SNR of 3, 10 and 20 dB, respectively. The order of the LMS and GALL filters was set to 31 (the same as the low-pass filter used to generate the additive MA components). For the LMS algorithm, the step size was set to 0.001; for the GALL filter, the forgetting factor λ was set to 1, and α 0. As shown in Fig. 5b, both the GALL and LMS filters can reduce the MA components from the synchronized respiratory signals. Compared with the LMS filter, the GALL filter has a faster convergence speed at every exercise level. Moreover, the GALL filter achieves almost the same convergence speed at different exercise levels. The LMS filter, however, shows different convergence speed at each exercise level. In this case (step size equals 0.001), the larger SNR, the slower the convergence speed. Therefore, in terms of the convergence speed, the GALL filter outperforms the LMS filter.

The performances of the MA cancellation, in terms of PR, SPI and SDR, for both the GALL filter and LMS filter, are shown in Table 1. According to the definition, PR is not an index for respiratory signal quality assessment, but an index for adaptive filtering performance evaluation. As shown in Table 1, both the GALL and LMS filters produce PRs larger than one in different exercise conditions, indicating that the MA components were reduced from the original respiratory signals. For SPI and SDR, according to the definitions, both SPI and SDR can be used as indices for respiratory signal quality evaluation. As shown in Table 1, SDR can quantify the respiratory signal quality effectively, and the larger SNR of the synchronized respiratory signals, the larger SDRs (SDR0). SPI, however, cannot reflect the respiratory signal quality correctly. The SPIs from both the GALL and LMS filters are extremely low. SPI was originally developed to evaluate the EEG signal quality, and it performed well in ECG-derived respiratory

Table 1 The performances of MA cancellation for the GALL and LMS filters with simulation data at different SNR levels

Parameters	SNR 3 dB			SNR 10 dB			SNR 20 dB		
	Pedalling	Jogging	Running	Pedalling	Jogging	Running	Pedalling	Jogging	Running
SDR0	0.668	0.663	0.665	0.909	0.907	0.908	0.990	0.989	0.989
SDR_GALL	0.999	0.999	0.999	0.999	0.999	0.999	0.999	0.999	0.999
SDR_LMS	0.998	0.998	0.998	0.995	0.996	0.996	0.994	0.995	0.995
PR_GALL	1.551	1.494	1.530	1.114	1.102	1.110	1.015	1.012	1.013
PR_LMS	1.524	1.474	1.509	1.106	1.095	1.104	1.006	1.007	1.007
SPI_GALL	0.068	0.091	0.119	0.095	0.120	0.136	0.117	0.135	0.143
SPI_LMS	0.092	0.104	0.076	0.091	0.087	0.099	0.064	0.096	0.097

SDR0: SDR for the MA-contaminated signals; SDR_GALL: SDR by the GALL filter; SDR_LMS: SDR by the LMS filter; PR_GALL: PR by the GALL filter; PR_LMS: PR by the LMS filter; SPI_GALL: SPI by the GALL filter; SPI_LMS: SPI by the LMS filter

signals [25]. For respiratory signals acquired by RIP, however, since more accurate respiratory waveform is recorded (see it in Fig. 5), the respiratory waveform is no longer smooth like a sinusoidal signal. SPI is suitable to evaluate the signal quality with only one frequency component. That explains why SPI lost its power for respiratory signals acquired by RIP technique. In this case, the parameter of SDR performed well and could represent the actual respiratory signal quality. Therefore, in the following sections, the indices of PR and SDR were used to assess the performance of the adaptive MA cancellation on actual respiratory signals acquired during exercise. SDR was also used as an optimization index to determine the parameters (α and λ) in the GALL filter.

From Table 1, it can also be seen that the GALL filter and LMS filter produce similar results in terms of both PR and SDR at different exercise levels. Both the GALL and LMS filters can improve the SDR effectively, indicating that adaptive filtering can improve the respiratory signal quality. Relatively, the GALL filter outperforms the LMS filter. The values of both PR and SDR from the GALL filter are a little higher than those from the LMS filter.

3.1.2 Respiration acquired during exercise

The parameters of the GALL filter (the number of lattice stages P, the pole location α and the forgetting factor λ) were determined as follows. The number of lattice stages, P, was set to 50. The value of P was chosen based on preliminary visual inspection of the maximum number of peaks in the spectra of a subset of the signals. Twofold cross validation was performed to determine the values of λ and α. The data records (totally 60 records from ten volunteers at six exercise levels) were randomly divided into two sets (d_0 and d_1), and both sets were equal size. We then trained on d_0 and tested on d_1, followed by training on d_1 and testing on d_0. These two parameters were jointly optimized for each GALL filter by maximizing the SDR of the training dataset. The maximization was performed over a predefined discrete set of values: for λ, this set was [0.5, 0.8415, 0.9749, 0.9960, 0.9994, 0.9999, 1] and for α, this set was 1–0.0005^i where i was linearly varied between 0 and 1 in 20 steps [33]. The key parameter for the unforced Kalman filter is the forgetting factor λ_K. In this study, the value of λ_K was set to 1, because values of $\lambda_K < 1$ led to deterioration of performance in terms of SDR.

Figure 6 shows an example of the MA cancellation by each GALL filter and the output of the Kalman filter. It can be seen that the best performance (with the largest values of PR and SDR) was achieved by the GALL filter with Axis II as the reference input. The unforced Kalman filter could track that channel and achieve a good performance. In this case, the performance of the combined Kalman filter is even better than any GALL filter.

Table 2 shows the performance statistics of the GALL and Kalman filters on the actual respiratory signals acquired at different activity levels. For each subject at each exercise level, we got three MA estimates by the three GALL filters. To test whether the Kalman filter can combine the outputs of the GALL filters to achieve robust MA estimation, at each exercise level, only the largest SDR among the three GALL filters was selected to calculate the group mean and standard deviation. The PR corresponding to the largest SDR at each exercise level was also selected and used to compute the mean value and standard deviation at each exercise stage. From Table 2 it can be seen that at low-level exercise intensity such as walking, slow and medium pedalling, SDR0 is high, meaning that there is not too much MA component residing in the respiratory signals. For activities at high intensity, SDR0 is relatively low, indicating that more MA components were introduced in the respiratory signals. At low-level exercise intensity of walking, slow and medium pedalling, the adaptive filter of both the GALL filter and

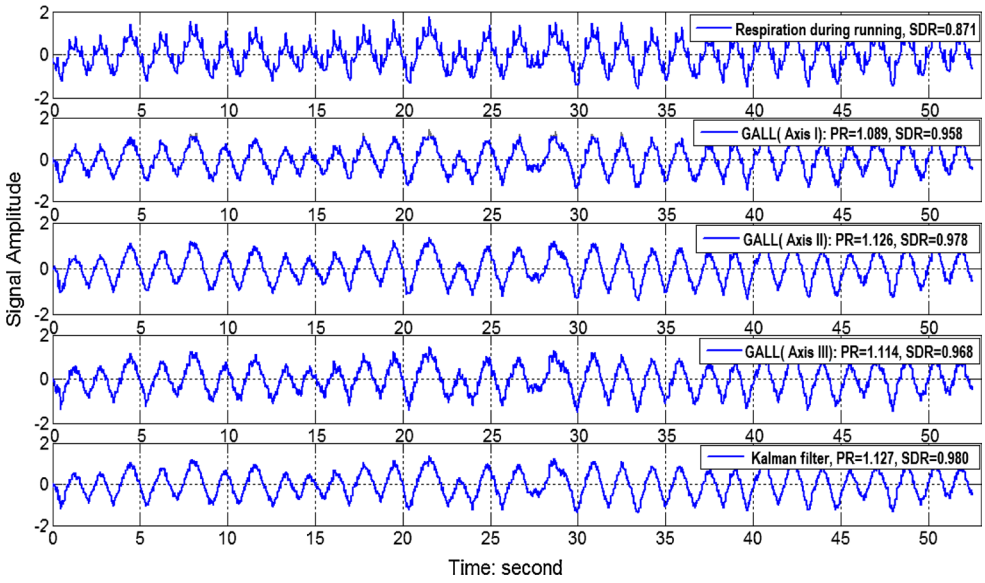

Fig. 6 Results of each GALL filter and the final Kalman filter during running

Table 2 Performance statistics of the GALL filter and Kalman filter at different activity levels

Parameters	Walking	Pedalling_slow	Pedalling_med	Pedalling_fast	Jogging	Running
SDR0	0.992 ± 0.008	0.993 ± 0.008	0.993 ± 0.005	0.978 ± 0.022	0.824 ± 0.120	0.768 ± 0.195
SDR_GALL	0.993 ± 0.010	0.991 ± 0.005	0.991 ± 0.005	0.987 ± 0.001	0.972 ± 0.014	0.956 ± 0.029
SDR_KF	0.989 ± 0.010	0.980 ± 0.015	0.985 ± 0.035	0.981 ± 0.008	0.973 ± 0.011	0.957 ± 0.025
PR_GALL	1.041 ± 0.036	1.052 ± 0.049	1.099 ± 0.115	1.131 ± 0.164	1.182 ± 0.139	1.313 ± 0.344
PR_KF	1.042 ± 0.038	1.054 ± 0.054	1.116 ± 0.193	1.218 ± 0.328	1.182 ± 0.138	1.308 ± 0.336

SDR0: SDR for the MA-contaminated signals; SDR_GALL: SDR by the GALL filter; SDR_KF: SDR by the Kalman filter; PR_GALL: PR by the GALL filter; PR_KF: PR by the Kalman filter

Kalman filter could not improve the respiratory signal quality further, because SDRs in this condition were originally high. In contrast, at high-level exercise intensity of jogging, fast pedalling and running, the adaptive filter of both the GALL filter and Kalman filter can improve the respiratory signal quality effectively.

3.2 Performance of MA cancellation in ECG signal

3.2.1 Simulation results

Figure 7a shows the original ECG, the synthesized signal with additive sine wave noise and Gaussian white noise, and the results of adaptive filtering using the LMS and GALL algorithms, respectively. It can be seen that relatively clean ECG signals can be recovered by both the GALL and LMS filters, even if the synthesized signal is completely ruined by the noise. From the recovered ECG signals, it can be seen that the GALL filter also performs better than the LMS filter (The same filter parameters used in respiratory signal simulation were employed in the LMS and GALL filters).

3.2.2 ECG acquired during exercise

The same filter structure of combing a bank of GALL filter and a Kalman filter was used to process the ECG signals acquired during exercise. For the ECG acquired in exercise, it was found that in some episodes and different types of noise can be introduced into the waveform, including baseline wonder, MA, EMG and some other high-frequency noise. In some other episodes, however, the signal quality is relatively good with less noise. Figure 8a shows an example of one segment of ECG waveform contaminated with noise during running. The result of adaptive MA reduction by the unforced Kalman filter is also presented. Figure 8b shows the power spectral densities of the original ECG signal, one axial output of the ACC signal and the output of the Kalman filter. It can be seen that compared with the original ECG, MA component was reduced by the adaptive filter. However, there is still some other noise component left. Therefore, signal quality of ECG was not improved effectively. Considering the fact that MA is not a dominant noise component in exercise ECG signals (Fig. 8b) and that signal quality cannot improve impressively (Fig. 8a), we

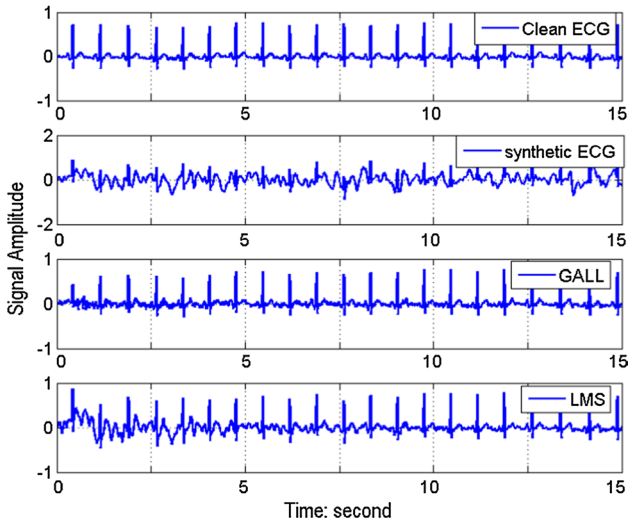

Fig. 7 Synthesized ECG and the results of adaptive filtering with LMS and GALL algorithms

did not perform any further statistical analysis on the adaptive MA filtering for ECG signals.

4 Discussions

For WHMSs, MA cancellation is a major challenge, as physiological signals may be contaminated by MA when these wearable systems are used in ambulatory conditions. In our study, it has been demonstrated that adaptive filtering with the ACC signal as the reference input can effectively reduce the MA component on respiratory signals. For WHMSs used in real life, because of the un-predictability of human body activities, robustness of MA cancellation should also be addressed. In this paper, a filter structure combining a bank of GALL filter and Kalman filter was proposed to achieve robust MA cancellation at different exercise levels. The major advantage of this structure is that it does not require supervised fine-tuning when the characteristic of the reference channel changes. This structure can be extended as a universal approach for other MA cancellation applications for WHMSs.

4.1 ACC outputs versus reference signals

Contrary to other studies [20, 29, 38], ECG signal quality could not be improved impressively by adaptive filtering with the ACC outputs as the reference signals. One most likely cause is that the way the sensor is placed in our system made it fail to capture the MA related information for ECG processing. Better adaptive filtering result might be achieved by integrating the ACC sensor into the electrodes to capture the electrode motion. However, in essence, MA on ECG waveform is generated from the change of biopotential by stretching the epidermis [26], while the signals captured by the ACC sensor are actually related with the physical movement. They are two different signals deriving from different mechanisms. That means there might be weak linear correlation between the noisy component presenting on ECG signal and the ACC signals. More noise components, such as baseline wander, EMG and other high-frequency noise, are not linearly correlated with the ACC signals. This factor may be the major reason that the adaptive filter with the ACC outputs as reference signals

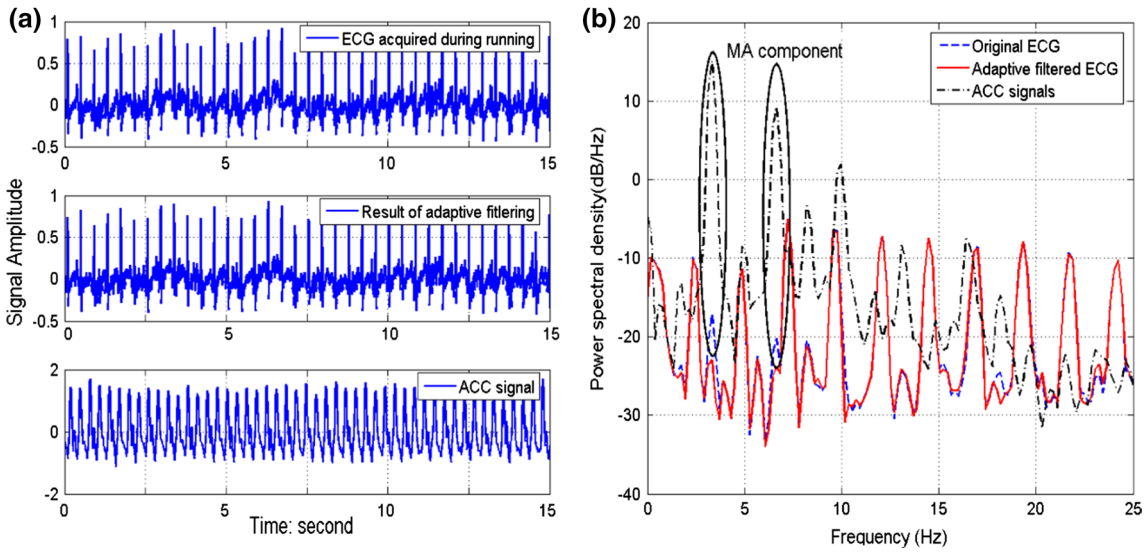

Fig. 8 **a** ECG signal acquired during running, result of adaptive filtering and one axial output of the ACC signal; **b** power spectral density of the original ECG, adaptive filtered ECG and the ACC signal

could not improve ECG signal quality effectively. For the respiratory signals recorded by RIP, as both the RIP and ACC sense MA from mechanical movement, ACC signals are highly correlated with the MA component in respiratory signals. Hence, the adaptive filter with the ACC outputs as the reference signals can reduce the MA component and improve the respiratory signal quality effectively.

4.2 MA modelling

In simulation studies, two strategies were tested for MA modelling in respiration and ECG signals, respectively. Theoretically, to remove the MA component from the corrupted signals, the reference signal should be correlated with the MA component. For this study, the correlation between the ACC signals and the MA component in respiratory signal was not quantified, but visually observed in most records. MA in physiological signal is usually caused by body movement, and accelerometer can capture body movement effectively; therefore, in our study, the outputs of the triaxial ACC were used as reference inputs to adaptive filter for the MA estimation. The results from both the simulation dataset and the actual dataset demonstrated the effectiveness of adaptive MA reduction in respiratory signals. For ECG signal, however, the correlation between the ACC signals and the MA component was not easy to be visually confirmed. Thus, instead of using the ACC output as the MA component, a presumed MA modelling of combing Gaussian white noise and a sine wave was used during the simulation. While the choice of Gaussian noise may seem unrealistic, it represents an ideal optimal case for testing our algorithm under a strict naive assumption of having an independent noise source between the ECG and the reference signals. For actual ECG, as aforementioned, there might be weak linear correlation between the noisy component and the ACC signals. As a result, the adaptive filter with the ACC outputs as the reference signals could not improve the ECG signal quality effectively.

4.3 Respiratory signal processing

Compared with other physiological signals, respiratory signals actually pose special challenges to adequate processing since MA component is common due to the physical activity, while the range of natural breathing frequency is relatively wide. Respiratory signal processing has not been studied sufficiently as other physiological signals such as ECG. Usually, a simple low-pass filter is used to separate respiratory signals from other high-frequency components, mainly for breathing rate detection. Although the low-pass filter can remove noise, it will also suppress important features at higher frequencies. Over-filtered respiratory signals may lose detailed structure and become too regular [40]. For some applications such as acute respiration and cough episodes, higher-frequency respiratory movements are of interest [9]. Meanwhile, respiration pattern or waveform morphology also carries information about health and diseases [23, 30], especially for research on cardio-respiratory interaction and evaluation of autonomic nervous system activity, which has been an area of interest for years [12, 27]. Compared with low-pass filters, adaptive filters are more likely used to recover the original shape of the respiratory waveform, and more accurate information can be acquired from the dynamically filtered respiratory signals.

4.4 Signal quality index

The research on signal quality index has been an area of interest for years now. For WHMSs, signal quality index is a useful tool to evaluate the quality of the waveforms acquired in ambulatory conditions. The concept of signal quality index was initially developed to quantify the physiological signal quality in intensive care unit to reduce false alarm rate and to improve the estimation of heart rate and blood pressure [4, 19]. Currently, most of the studies are focused on the ECG signal quality evaluation. Methods to assess the respiratory signal quality are not widely available. In our study, it was found that the SPI based signal quality index is not good for the RIP respiratory signal quality evaluation. The SDR-based signal quality index can be used to assess the amount of the noise component residing in the respiratory signals. From Fig. 1 and Table 2, it can be seen that for RIP respiration, there is not too much MA component during walking, slow and medium pedalling. The original SDRs during walking, slow and medium pedalling are very high. For high-intensity movement, the SDRs are low, and the respiratory signal quality can be improved effectively by adaptive filtering. It is also worth mentioning that even though SDR is a better index than SPI for RIP respiratory signal quality evaluation, SDR is not a perfect index for adaptive filter performance evaluation. In essence, SDR is a suitable index for band-pass filter performance evaluation. That might be the reason that during low-intensity exercise, such as walking, slow and medium pedalling, the SDRs achieved by the adaptive filter were even lower than the original SDRs. The signal quality of the respiratory signals during walking, slow and medium pedalling might also have been improved by the adaptive filter. However, it may not be reflected by the SDR index. A more robust and effective respiratory signal quality index should be developed and evaluated in the future.

It should also be noted that the structure of the adaptive filter used in this paper can be extended to other physiological signals acquired in ambulatory conditions for robust MA cancellation, such as PPG and phonocardiogram, as well as respiratory signals acquired by other techniques.

For respiration acquired by impendence plethysmography, more work needs to be done to check the validation of our approach as the mechanism behind impendence plethysmography is different from RIP.

5 Conclusions

This paper demonstrates that MA component in both respiratory and ECG signals can be reduced by a proposed adaptive filter with ACC signals as reference input. The structure of the adaptive filter by combining a bank of GALL filter and an unforced Kalman filter can achieve robust MA cancellation without supervised selection of reference channel. For respiratory signals, signal quality can be improved effectively through the MA reduction. For ECG signals, contrary to prior work [20, 29, 38], as the MA is not a dominant noise component, signal quality could not be enhanced effectively by the adaptive MA cancellation.

Acknowledgments This project was supported by Beijing Natural Science Foundation (Grant Numbers: 3102028, 3122034) and General Logistics Science Foundation (Grant Number: CWS11C108). The work was also funded in part by the National Institute of Biomedical Imaging and Bio-engineering and by the National Institute of General Medical Sciences, under NIH cooperative agreement U01-EB-008577 and NIH grant R01- EB001659.

References

1. Benesty J, Huang Y (2003) Adaptive signal processing: applications to real-world problems. Springer, Berlin, pp 129–153
2. Black AM, Bambridge A, Kunst G, Millard RK (2001) Progress in non-invasive respiratory monitoring using uncalibrated breathing movement components. Physiol Meas 22(1):245–261
3. Chen L, McKenna T, Reisner A, Reifman J (2006) Algorithms to qualify respiratory data collected during the transport of trauma patients. Physiol Meas Sep 27(9):797–816
4. Clifford GD, Behar J, Li Q, Rezek I (2012) Signal quality indices and data fusion for determining clinical acceptability of electrocardiograms. Physiol Meas Sep 33(9):1419–1433
5. Cohen KP, Ladd WM, Beams DM, Sheers WS, Radwin RG, Tompkins WJ, Webster JG (1997) Comparison of impedance and inductance ventilation sensors on adults during breathing, motion, and simulated airway obstruction. IEEE Trans Biomed Eng 44(7):555–566
6. Coyle S, Lau KT, Moyna N, O'Gorman D, Diamond D, Di Francesco F, Costanzo D, Salvo P, Trivella MG, De Rossi DE, Taccini N, Paradiso R, Porchet JA, Ridolfi A, Luprano J, Chuzel C, Lanier T, Revol-Cavalier F, Schoumacker S, Mourier V, Chartier I, Convert R, De-Moncuit H, Bini C (2010) BIOTEX—biosensing textiles for personalised healthcare management. IEEE Trans Inf Technol Biomed 14(2):364–370
7. Dowling AV, Favre J, Andriacchi TP (2011) A wearable system to assess risk for anterior cruciate ligament injury during jump landing: measurements of temporal events, jump height, and sagittal plane kinematics. J Biomech Eng 133(7):071008
8. Fejzo Z, Lev-Ari L (1997) Adaptive Laguerre-lattice filters. IEEE Trans Signal Process 45(12):3006–3016
9. Fiamma MN, Samara Z, Baconnier P, Similowski T, Straus C (2007) Respiratory inductive plethysmography to assess respiratory variability and complexity in humans. Respir Physiol Neurobiol 156(2):234–239
10. Frank TH, Blaumanis OR, Chen SH, Petrie RH, Gibbs RK, Wells RL, Johnson TR (1992) Noninvasive fetal ECG mode fetal heart rate monitoring by adaptive digital filtering. J Perinat Med 20(2):93–100
11. Goldman JM, Petterson MT, Kopotic RJ, Barker SJ (2000) Masimo signal extraction pulse oximetry. J Clin Monit Comput 16(7):475–483
12. Grossman P, Wilhelm FH, Spoerle M (2004) Respiratory sinus arrhythmia, cardiac vagal control, and daily activity. Am J Physiol Heart Circ Physiol 287(2):H728–H734
13. Han H, Kim J (2012) Artifacts in wearable photoplethysmographs during daily life motions and their reduction with least mean square based active noise cancellation method. Comput Biol Med 42(4):387–393
14. Haykin S (2001) Adaptive filter theory, 4th edn. Prentice-Hall, Upper Saadle River, pp 485–495
15. Iyer VK, Ploysongsang Y, Ramamoorthy PA (1990) Adaptive filtering in biological signal processing. Crit Rev Biomed Eng 17(6):531–584
16. Keenan DB, Wilhelm FH (2005) Adaptive and wavelet filtering methods for improving accuracy of respiratory measurement. Biomed Sci Instrum 41:37–42
17. Lanatà A, Scilingo EP, Nardini E, Loriga G, Paradiso R, De-Rossi D (2010) Comparative evaluation of susceptibility to motion artifact in different wearable systems for monitoring respiratory rate. IEEE Trans Inf Technol Biomed 14(2):378–386
18. Lee B, Han J, Baek HJ, Shin JH, Park KS, Yi WJ (2010) Improved elimination of motion artifacts from a photoplethysmographic signal using a Kalman smoother with simultaneous accelerometry. Physiol Meas 31(12):1585–1603
19. Li Q, Mark RG, Clifford GD (2008) Robust heart rate estimation from multiple asynchronous noisy sources using signal quality indices and a Kalman filter. Physiol Meas 29(1):15–32
20. Liu SH (2011) Motion artifact reduction in electrocardiogram using adaptive filter. J Med Biol Eng 31(1):67–72
21. Liu Y, Pecht MG (2011) Reduction of motion artifacts in electrocardiogram monitoring using an optical sensor. Biomed Instrum Technol 45(2):155–163
22. Martens SM, Mischi M, Oei SG, Bergmans JW (2006) An improved adaptive power line interference canceller for electrocardiography. IEEE Trans Biomed Eng 53(11):2220–2231
23. Masaoka Y, Homma I (1997) Anxiety and respiratory patterns: their relationship during mental stress and physical load. Int J Psychophysiol 27(2):153–159
24. Mundt CW, Montgomery KN, Udoh UE, Barker VN, Thonier GC, Tellier AM, Ricks RD, Darling RB, Cagle YD, Cabrol NA, Ruoss SJ, Swain JL, Hines JW, Kovacs GT (2005) A multiparameter wearable physiologic monitoring system for space and terrestrial applications. IEEE Trans Inf Technol Biomed 9(3):382–391
25. Nemati S, Malhotra A, Clifford GD (2010) Data fusion for improved respiration rate estimation. http://dspace.mit.edu/openaccess-disseminate/1721.1/67021
26. Odman S, Oberg P (1982) Movement induced potentials in surface electrodes. Med Eng Comput 20:159–166
27. Pereda E, De la Cruz DM, De Vera L, González JJ (2005) Comparing generalized and phase synchronization in cardiovascular and cardiorespiratory signals. IEEE Trans Biomed Eng 52(4):578–583
28. Poh MZ, Swenson NC, Picard RW (2010) Motion-tolerant magnetic earring sensor and wireless earpiece for wearable photoplethysmography. IEEE Trans Inf Technol Biomed 14(3):786–794

29. Raya MAD, Sison LG (2002) Adaptive noise cancelling of motion artifact in stress ECG signals using accelerometer. Annual International Conference of the IEEE Engineering in Medicine and Biology Society-EMBC, IEEE 2:1756–1757
30. Ritz T, Simon E, Trueba AF (2011) Stress-induced respiratory pattern changes in asthma. Psychosom Med 73(6):514–521
31. Rutherford JJ (2010) Wearable technology. Health-care solutions for a growing global population. IEEE Eng Med Biol Mag 29(3):19–24
32. Ryan KL, Rickards CA, Hinojosa-Laborde C, Gerhardt RT, Cain J, Convertino VA (2011) Advanced technology development for remote triage applications in bleeding combat casualties. US Army Med Dep J 2:61–72
33. Silva I, Lee J, Mark RG (2012) Signal quality estimation with multichannel adaptive filtering in intensive care settings. IEEE Trans Biomed Eng 59(9):2476–2485
34. Sörnmo L, Laguna P (2005) Bioelectrical signal processing in cardiac & neurological applications. Elsevier Academic, Burlington, pp 98–103
35. Such O (2007) Motion tolerance in wearable sensors—the challenge of motion artifact. Conf Proc IEEE Eng Med Biol Soc. IEEE, Lyon, pp 1542–1545
36. Teng XF, Zhang YT, Poon CC, Bonato P (2008) Wearable medical systems for p-Health. IEEE Rev Biomed Eng 1:62–74
37. Thakor NV, Zhu YS (1991) Applications of adaptive filtering to ECG analysis: noise cancellation and arrhythmia detection. IEEE Trans Biomed Eng 38(8):785–794
38. Tong DA, Bartels KA, Honeyager KS (2002) Adaptive reduction of motion artifact in the electrocardiogram. In: annual international conference of the IEEE Engineering in Medicine and Biology Society-EMBC, IEEE, 2:1403–1404
39. Widrow B, Glover JR Jr, McCool JM, Kaunitz J, Williams CS, Hearn RH, Zeidler JR, Dong E Jr, Goodlin RC (1975) Adaptive noise cancelling: principles and applications. Proc of the IEEE 63(12):1695–1716
40. Wu MC, Hu CK (2006) Empirical mode decomposition and synchrogram approach to cardiorespiratory synchronization. Phys Rev E 73(5):051917
41. Yan YS, Zhang YT (2008) An efficient motion-resistant method for wearable pulse oximeter. IEEE Trans Inf Technol Biomed 12(3):399–405
42. Zhang ZB, Yu MS, Li RX, Wu TH, Wu JL (2006) Design of a wearable respiratory inductive plethysmograph and its applications. Space Med Med Eng 19:377–381
43. Zhang YT, Liu Q, Poon CCY, Zheng YL, Gao H (2011) Cardiovascular health informatics: wearable intelligent sensors for e-health (WISE). In: 2011 IEEE technology time machine symposium on technologies beyond 2020 (TTM). IEEE, Hong Kong, p 1
44. Zhang ZB, Shen YH, Wang WD, Wang BQ, Zheng JW (2011) Design and implementation of sensing shirt for ambulatory cardiopulmonary monitoring. J Med Bio Eng 31(3):207–215